

Forward modelling of geophysical electromagnetic data on unstructured grids using a finite-volume approach

Hormoz Jahandari and Colin G. Farquharson



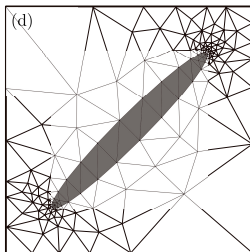
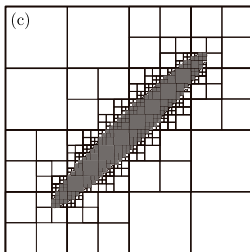
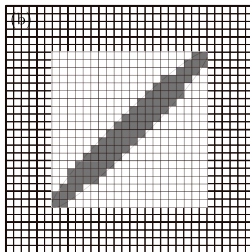
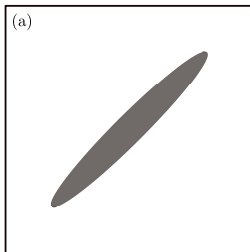
Memorial University
Department of Earth Sciences
St. John's, Newfoundland, Canada

76th EAGE Conference & Exhibition, Amsterdam
June 18, 2014

- 1 Unstructured grids
- 2 Finite-volume discretization of Maxwell's equations (direct EM-field and potential formulation)
- 3 Example for magnetic dipole sources
- 4 Example for a long grounded wire source
- 5 Example for a helicopter EM survey
- 6 Conclusions

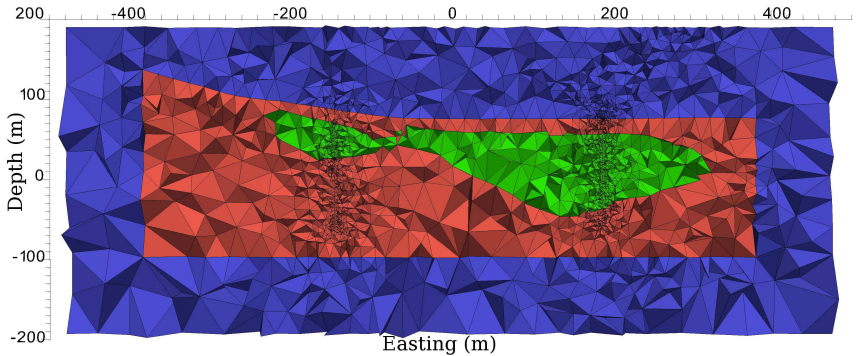
Unstructured grids

- Model irregular structures



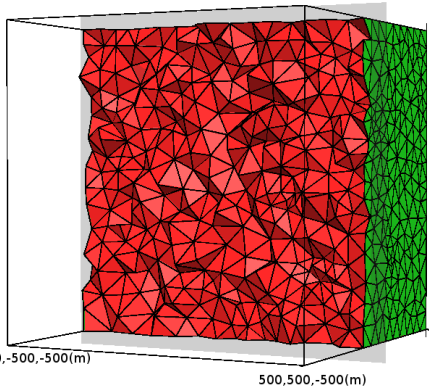
Unstructured grids

- Topographical features
- Geological interfaces
- Local refinement (at observation points, sources, interfaces)

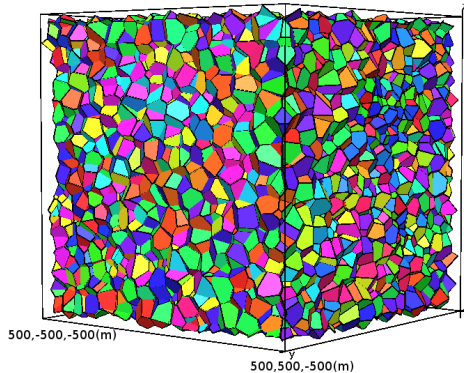


Dual tetrahedral-Voronoi grids

- Grid generator: TetGen (Si, 2004)



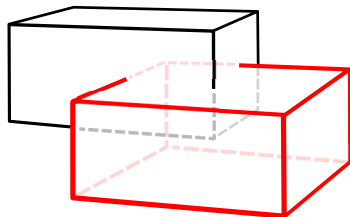
tetrahedral grid



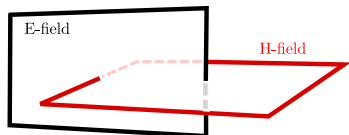
Voronoi grid

Staggered finite-volume schemes

- Magnetic field divergence free
- Easy for implementing boundary conditions
- Satisfies the continuity of tangential E
- Physically meaningful

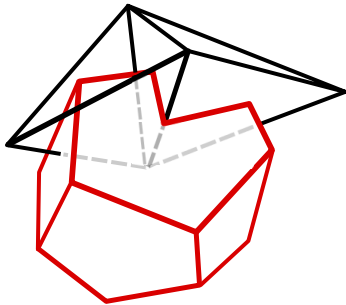


Rectilinear dual grid

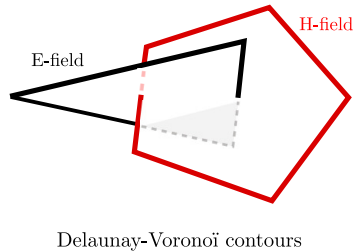


Rectilinear dual contours

Staggered finite-volume schemes



Dual tetrahedral-Voronoi grid



Delaunay-Voronoi contours

Staggered finite-volume schemes

Direct EM-field method

- Unknowns are E and/or H
- Simpler
- Smaller system of equations
- Ill-conditioned

EM Potential ($A - \phi$) method

- Unknowns are A and ϕ
- Larger system of equations
- Well-conditioned
- Allows studying the galvanic and inductive parts

- **Maxwell's equations:**

$$\nabla \times \mathbf{E} = -i\omega\mu_0\mathbf{H} - i\omega\mu_0\mathbf{M}_p$$

$$\nabla \times \mathbf{H} = \sigma\mathbf{E} + \mathbf{J}_p$$

Helmholtz equation for electric field

$$\nabla \times \nabla \times \mathbf{E} + i\omega\mu_0\sigma\mathbf{E} = -i\omega\mu_0\mathbf{J}_p - i\omega\mu_0(\nabla \times \mathbf{M}_p)$$

- **Homogeneous Dirichlet boundary condition:**

$$\mathbf{E} = 0 \quad \text{at } \infty$$

or

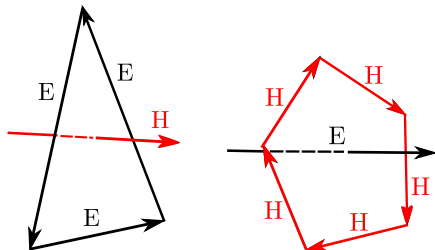
$$\mathbf{E} \cdot \boldsymbol{\tau} = 0 \quad \text{on } \Gamma$$

EM-field formulation: Discretization

- Integral form of Maxwell's equations:

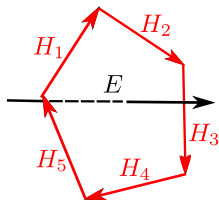
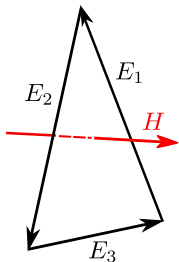
$$\oint_{\partial S^D} \mathbf{E} \cdot d\mathbf{l}^D = -i\mu_0\omega \iint_{S^D} \mathbf{H} \cdot d\mathbf{S}^D - i\mu_0\omega \iint_{S^D} \mathbf{M}_p \cdot d\mathbf{S}^D$$

$$\oint_{\partial S^V} \mathbf{H} \cdot d\mathbf{l}^V = \sigma \iint_{S^V} \mathbf{E} \cdot d\mathbf{S}^V + \iint_{S^V} \mathbf{J}_p \cdot d\mathbf{S}^V$$



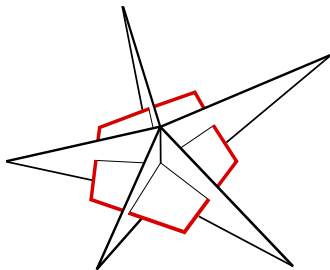
- Discretized form of Maxwell's equations:

$$\sum_{q=1}^{w_j^D} E_{i(j,q)} I_{i(j,q)}^D = -i\mu_0\omega H_j S_j^D - i\mu_0\omega M_{p_j} S_j^D$$
$$\sum_{k=1}^{w_i^V} H_{j(i,k)} I_{j(i,k)}^V = \sigma E_i S_i^V + J_{p_i} S_i^V.$$



- Discretized form of Helmholtz equation:

$$\sum_{k=1}^{W_i^V} \left(\left(\sum_{q=1}^{W_j^D} E_{i(j,q)} I_{i(j,q)}^D \right) \frac{I_{j(i,k)}^V}{S_{j(i,k)}^D} \right) + i\omega\mu_0\sigma E_i S_i^V$$
$$= -i\omega\mu_0 \sum_{k=1}^{W_i^V} M_{pj(i,k)} \frac{I_{j(i,k)}^V}{S_{j(i,k)}^D} - i\omega\mu_0 J_{p_i}$$



EM potential (\mathbf{A} - ϕ) formulation of Maxwell's equations

- Magnetic vector and electric scalar potentials:

$$\mathbf{E} = -i\omega\mathbf{A} - \nabla\phi$$
$$\mu_0\mathbf{H} = \nabla \times \mathbf{A}$$

Helmholtz equation in terms of potentials with Coulomb gauge

$$\nabla \times \nabla \times \mathbf{A} - \nabla(\nabla \cdot \mathbf{A}) + i\omega\mu_0\sigma\mathbf{A} + \sigma\mu_0\nabla\phi = \mu_0\mathbf{J}_p + \mu_0\nabla \times \mathbf{M}_p$$

Conservation of charge

$$-\nabla \cdot \mathbf{J} = \nabla \cdot \mathbf{J}_p$$
$$i\omega\nabla \cdot \sigma\mathbf{A} + \nabla \cdot \sigma\nabla\phi = \nabla \cdot \mathbf{J}_p$$

- Homogeneous Dirichlet boundary condition:

$$(\mathbf{A}, \phi) = 0 \quad \text{at } \infty$$

or

$$(\mathbf{A} \cdot \boldsymbol{\tau}, \phi) = 0 \quad \text{on } \Gamma$$

EM potential (\mathbf{A} - ϕ) formulation of Maxwell's equations

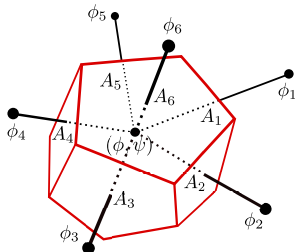
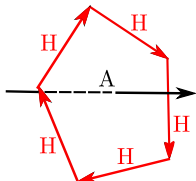
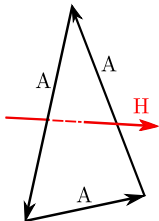
Relations used for the finite-volume discretization

$$\nabla \times \mathbf{H} - \mu_0^{-1} \nabla \psi + i\omega \sigma \mathbf{A} + \sigma \nabla \phi = \mathbf{J}_p + \nabla \times \mathbf{M}_p \quad (1)$$

$$\mu_0 \mathbf{H} = \nabla \times \mathbf{A} \quad (2)$$

$$\psi = \nabla \cdot \mathbf{A} \quad (3)$$

$$i\omega \nabla \cdot \sigma \mathbf{A} + \nabla \cdot \sigma \nabla \phi = \nabla \cdot \mathbf{J}_p \quad (4)$$



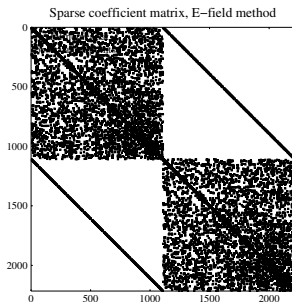
The system of equations for the direct method

- Decompose E into real and imaginary parts:

$$E = E_{re} + iE_{im}$$

- Resulting block matrix equation:

$$\begin{pmatrix} \mathbf{A} & -\mathbf{B} \\ \mathbf{B} & \mathbf{A} \end{pmatrix} \begin{pmatrix} \mathbf{E}_{re} \\ \mathbf{E}_{im} \end{pmatrix} = \begin{pmatrix} 0 \\ \mathbf{S}_{re} \end{pmatrix}$$



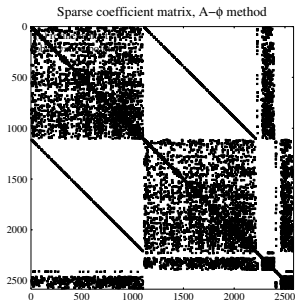
The system of equations for the A- ϕ method

- Decompose \mathbf{A} and ϕ into real and imaginary parts:

$$\mathbf{A} = \mathbf{A}_{re} + i\mathbf{A}_{im} ; \phi = \phi_{re} + i\phi_{im}$$

- Resulting block matrix equation:

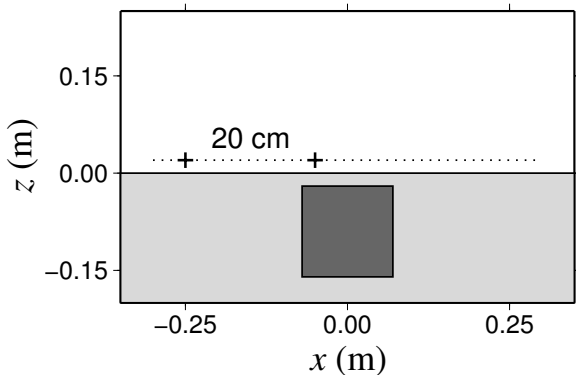
$$\begin{pmatrix} \mathbf{A} & -\omega\mathbf{B} & \mathbf{C} & 0 \\ \omega\mathbf{B} & \mathbf{A} & 0 & -\mathbf{C} \\ 0 & -\omega\mathbf{D} & \mathbf{E} & 0 \\ \omega\mathbf{D} & 0 & 0 & \mathbf{E} \end{pmatrix} \begin{pmatrix} \mathbf{A}_{re} \\ \mathbf{A}_{im} \\ \Phi_{re} \\ \Phi_{im} \end{pmatrix} = \begin{pmatrix} \mathbf{S}_1 \\ 0 \\ \mathbf{S}_2 \\ 0 \end{pmatrix}$$



- **Direct EM-field method: MUMPS sparse direct solver (Amestoy et. al, 2006)**
- **EM Potential method: BCGSTAB iterative solver from SPARSKIT (Saad, 1990)**

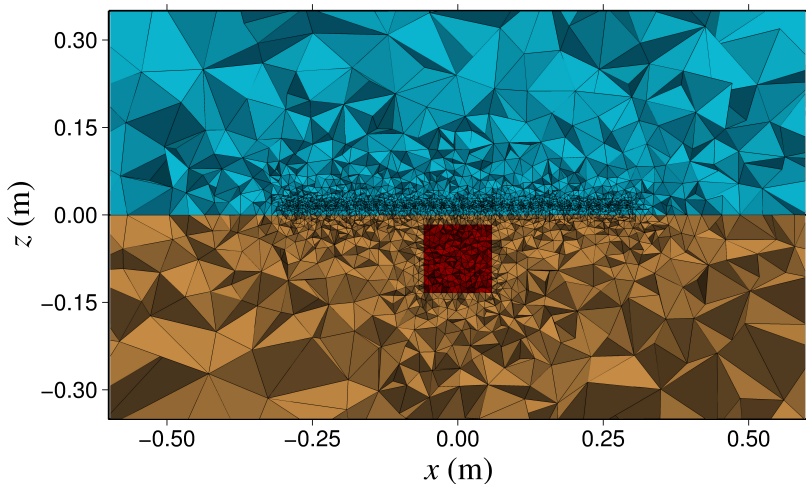
Example 1: magnetic dipole transmitter-receiver pairs

- Graphite cube in brine (physical scale modelling measurements)
- Transmitter-receiver pairs along the x axis at $z = 2 \text{ cm}$
- Dimensions of the cubic graphite: $14 \times 14 \times 14 \text{ cm}$
- $\sigma_{brine} = 7.3 \text{ S/m}$; $\sigma_{prism} = 63,000 \text{ S/m}$
- Frequencies: 1, 10, 100, 200, 400 kHz



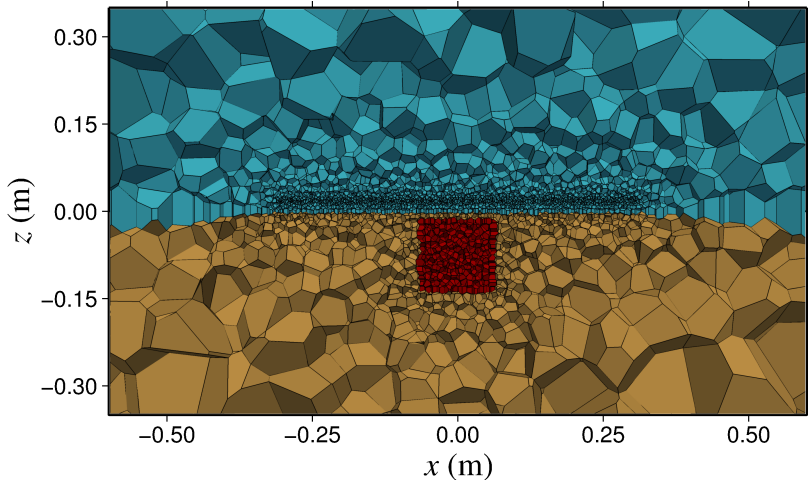
Example 1: magnetic dipole transmitter-receiver pairs

- Grid refined at the sources, observation points and the prism



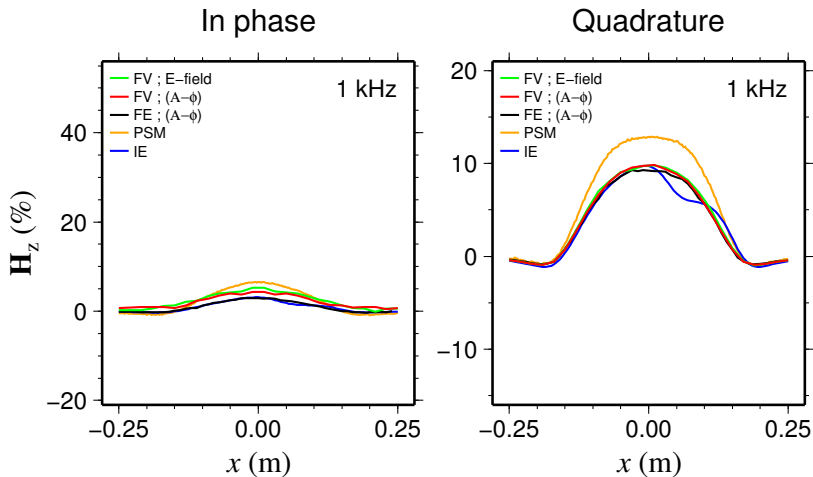
Example 1: magnetic dipole transmitter-receiver pairs

- Grid refined at the sources, observation points and the prism



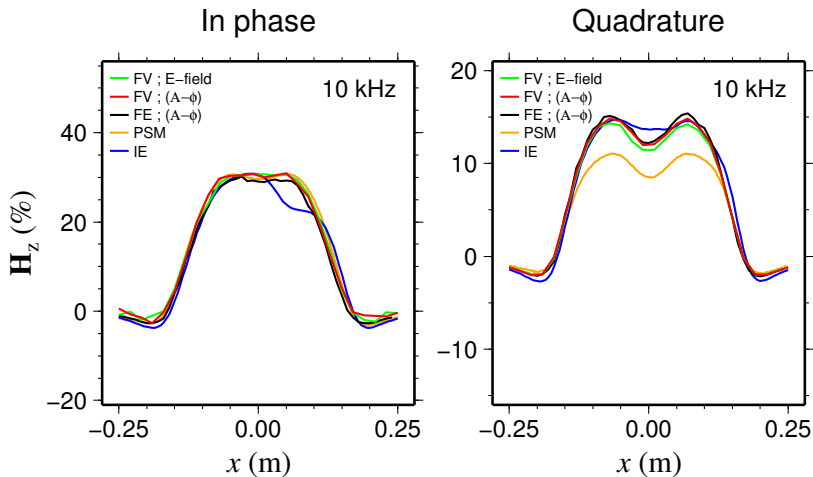
Example 1: magnetic dipole transmitter-receiver pairs

- Scattered H-field: (total–free-space)/free-space



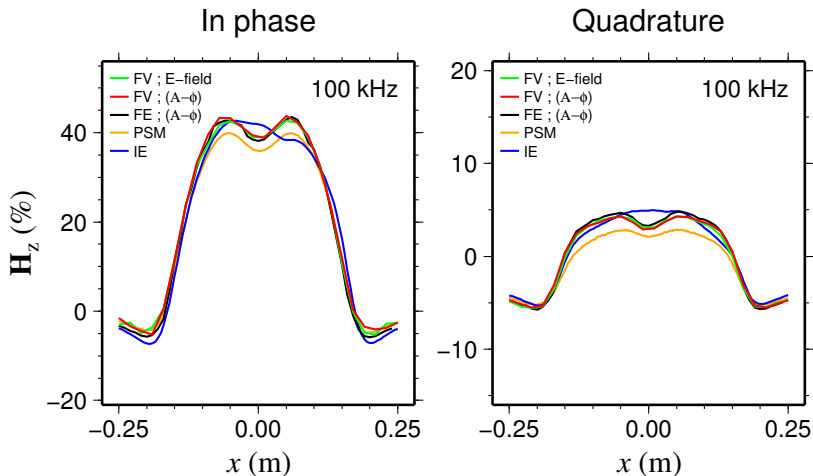
Example 1: magnetic dipole transmitter-receiver pairs

- Scattered H-field: $(\text{total} - \text{free-space}) / \text{free-space}$



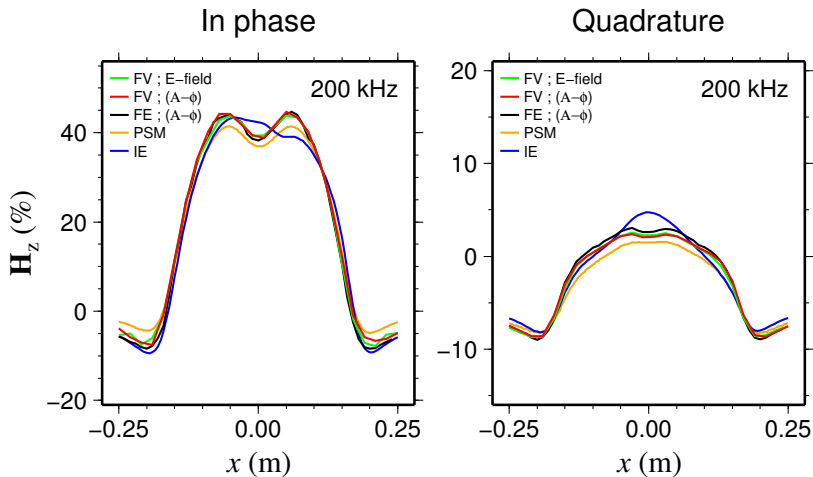
Example 1: magnetic dipole transmitter-receiver pairs

- Scattered H-field: $(\text{total} - \text{free-space}) / \text{free-space}$



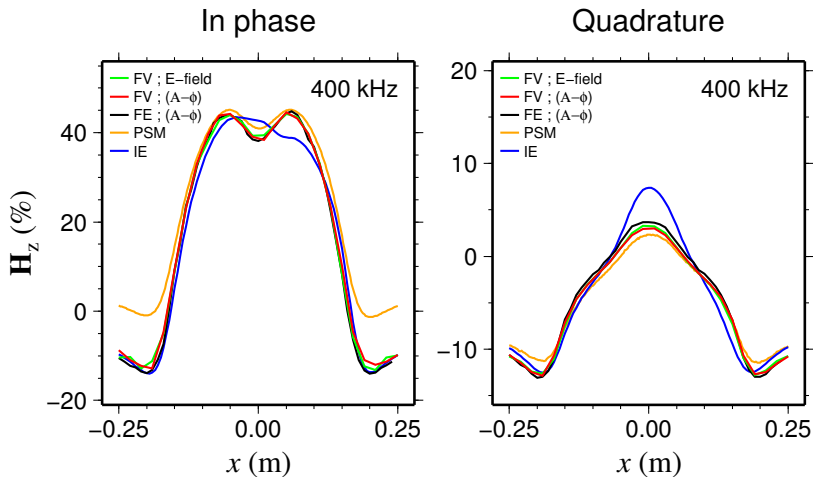
Example 1: magnetic dipole transmitter-receiver pairs

- Scattered H-field: $(\text{total} - \text{free-space}) / \text{free-space}$



Example 1: magnetic dipole transmitter-receiver pairs

- Scattered H-field: $(\text{total} - \text{free-space}) / \text{free-space}$

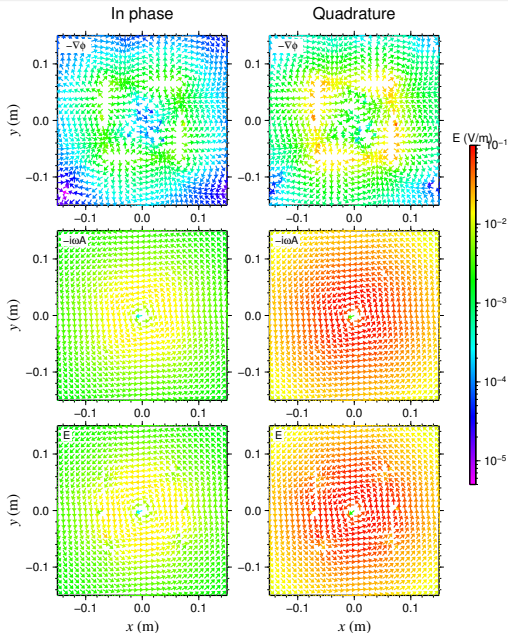


Example 1: magnetic dipole transmitter-receiver pairs

- Galvanic part ($-\nabla\phi$)

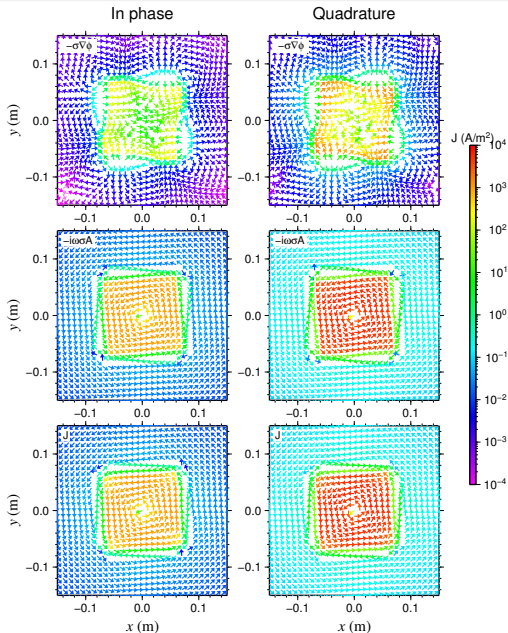
- Inductive part ($-i\omega A$)

- Total electric field:
 $E = -\nabla\phi - i\omega A$



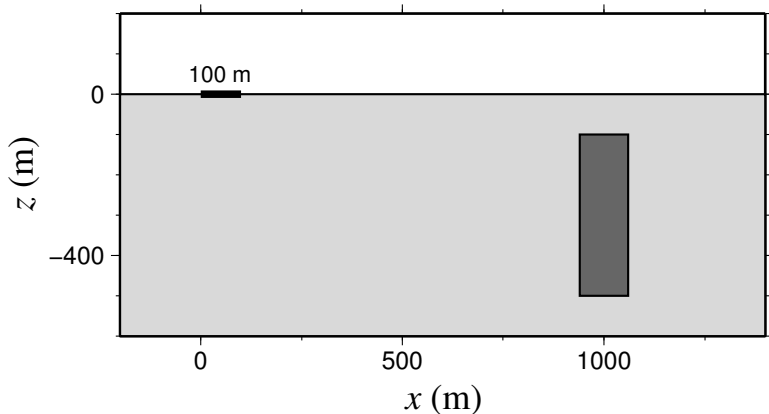
Example 1: magnetic dipole transmitter-receiver pairs

- Galvanic part ($-\sigma\nabla\phi$)
- Inductive part ($-i\omega\sigma A$)
- Total current density:
 $J = -\sigma\nabla\phi - i\omega\sigma A$



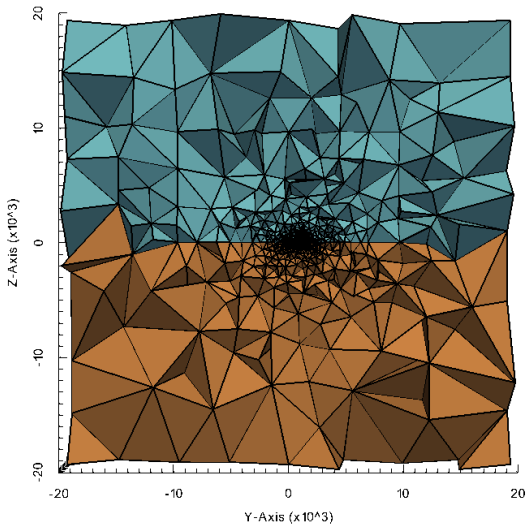
Example 2: long grounded wire

- 100 m wire along the x axis operating at 3 Hz
- Dimensions of the prism: $120 \times 200 \times 400$ m
- $\sigma_{ground} = 0.02$ S/m ; $\sigma_{prism} = 0.2$ S/m
- Observation points along the x axis



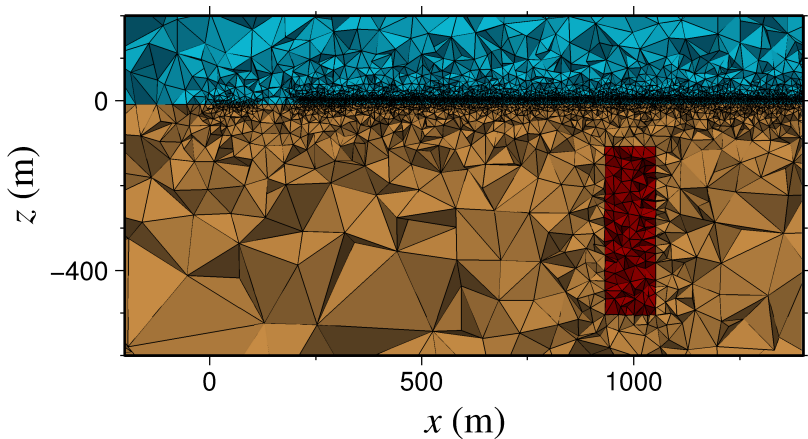
Example 2: long grounded wire

- Dimensions of the domain: $40 \times 40 \times 40$ km
- Number of tetrahedra: 162,689



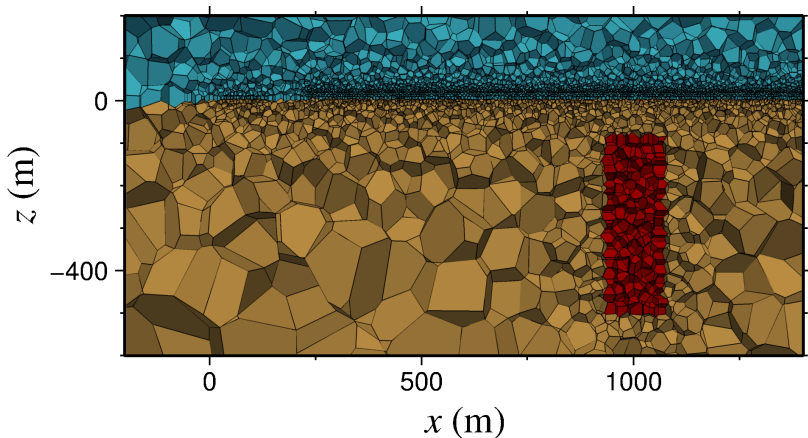
Example 2: long grounded wire

- EM-field method: MUMPS (40 s ; memory 4 Gbytes)
- (on Apple Mac Pro; 2.26 GHz Quad-Core Intel Xeon processor)



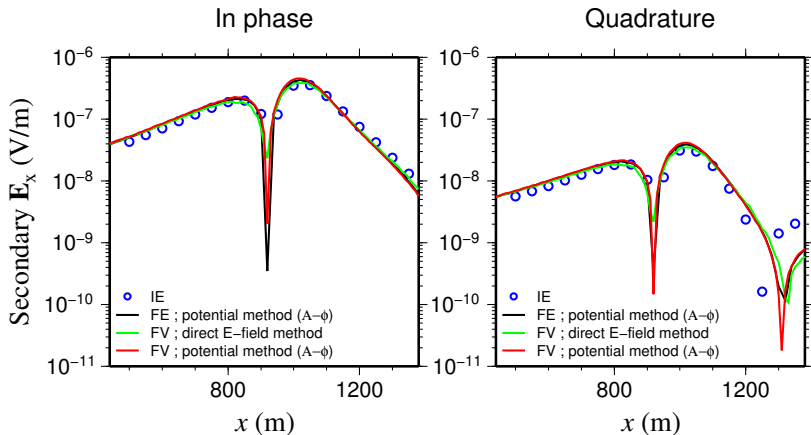
Example 2: long grounded wire

- Potential method: BCGSTAB with $l_{fil}=3$ and ILUT preconditioner (345 s ; memory 0.8 Gbytes ; 2000 iterations ; residual norm 10^{-12})
- (on Apple Mac Pro; 2.26 GHz Quad-Core Intel Xeon processor)



Example 1: long grounded wire

- Scattered electric field

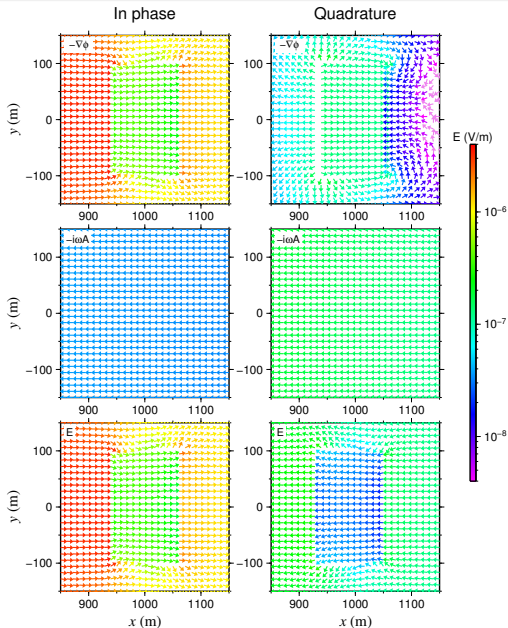


Example 2: long grounded wire

- Galvanic part ($-\nabla\phi$)

- Inductive part ($-i\omega A$)

- Total electric field:
 $E = -\nabla\phi - i\omega A$

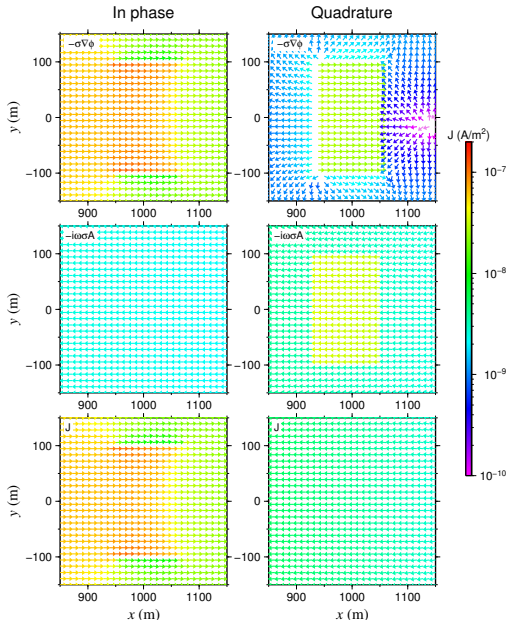


Example 2: long grounded wire

- Galvanic part ($-\sigma\nabla\phi$)

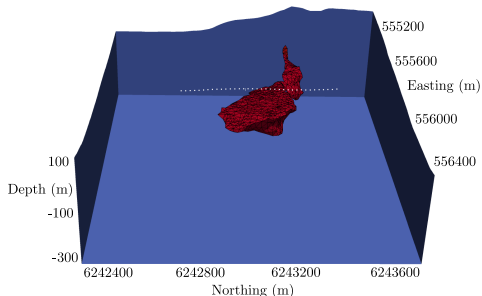
- Inductive part ($-i\omega\sigma A$)

- Total current density:
 $J = -\sigma\nabla\phi - i\omega\sigma A$



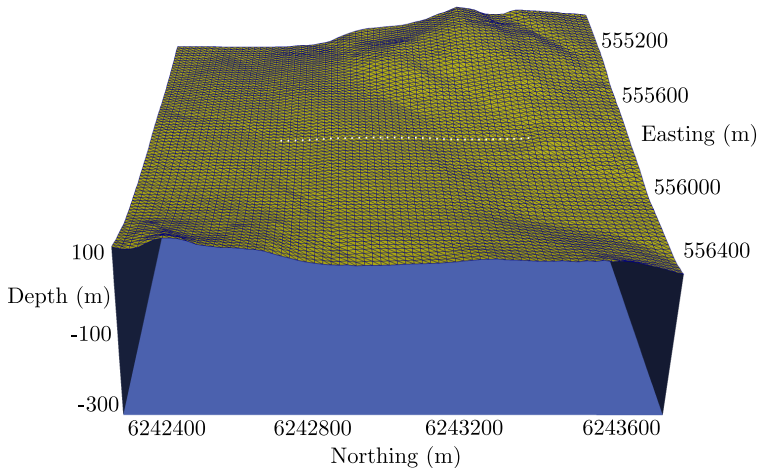
Example 3: Ovoid, HEM survey (direct method)

- Ovoid: massive sulfide ore body, Voisey's Bay, Labrador, Canada
- HEM survey of the region has been simulated
- Transmitter and receiver towed below the helicopter 30 m above ground
- Transmitter-receiver separation was 8 m and the frequency was 900 Hz
- $\sigma_{ground} = 0.001$ and $\sigma_{ovoid} = 100$ S/m were chosen by try-and-error
- Number of tetrahedra: 190,121; Number of unknowns: 223,650



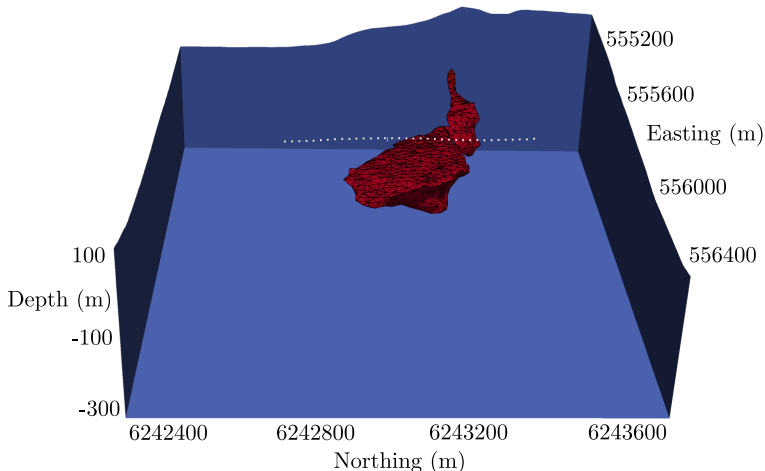
Example 3: Ovoid, HEM survey (direct method)

- Topography of the region



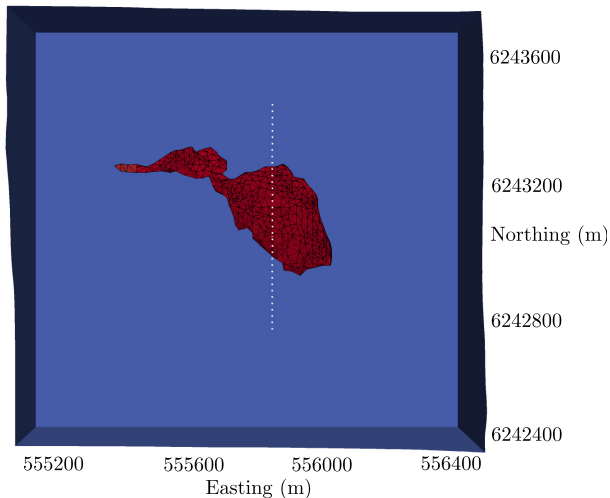
Example 3: Ovoid, HEM survey (direct method)

- White dots show the observation points



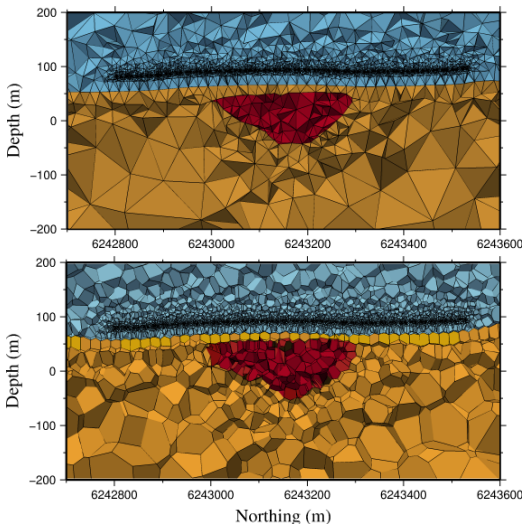
Example 3: Ovoid, HEM survey (direct method)

- The plan view



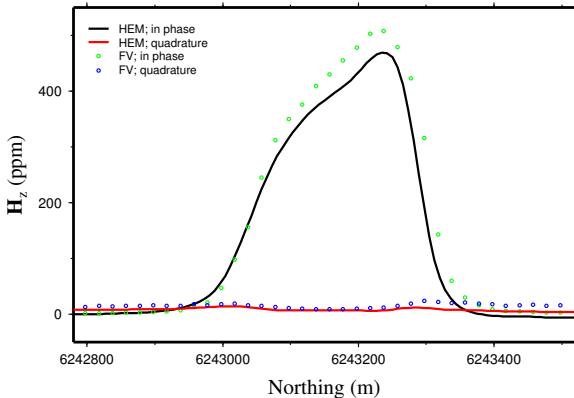
Example 3: Ovoid, HEM survey (direct method)

- Grid refined at the sources and observation points



Example 3: Ovoid, HEM survey (direct method)

- FV results (circles) vs real HEM data (lines)



- A finite-volume approach is used for modelling the total field EM data. This method uses the staggered tetrahedral-Voronoi grids.
- The aim is to make use of the features of unstructured grids for efficient modeling of the subsurface and for local refinements in the grid.
- Both the direct EM-field formulation and the potential formulation of Maxwell's equation are discretized and solved using a sparse direct solver (MUMPS) and an iterative solver (BCGSTAB).
- The schemes have been tested for two models with simple geometries: one with a long grounded wire source and a small conductivity contrast; another one for magnetic source-receiver pairs with large conductivity contrast.
- For the both examples, the results from the two FV schemes are in good agreement with those from the literature.

- The direct EM-field scheme is ill-conditioned and it can not be easily solved using the iterative solvers. The only option is using a direct solver. The $A - \phi$ scheme, in the other hand, is better conditioned and it can be solved using iterative solvers.
- An example is also included in which helicopter-borne EM data is simulated for a model with irregular geometry and with topography. The results from the direct EM-field method show good agreement with the real data.

Acknowledgements

- ACOA
(Atlantic Canada Opportunities Agency)
- NSERC
(Natural Sciences and Engineering Research Council of Canada)
- Vale



Atlantic Canada
Opportunities
Agency



NSERC
CRSNG



VALE

- Amestoy, P. R., Guermouche, A., L'Excellent, J. -Y. and S. Pralet, 2006. Hybrid scheduling for the parallel solution of linear systems, *Parallel Computing*, 32, 136156.
- Ansari, S. M., and C. G. Farquharson, 2013, Three-dimensional modeling of controlled-source electromagnetic response for inductive and galvanic components: Presented at the 5th International Symposium on Three-Dimensional Electromagnetics.
- Farquharson, C. G., and D. W. Oldenburg, 2002, An integral-equation solution to the geophysical electromagnetic forward-modelling problem, in *Three-Dimensional Electromagnetics: Proceedings of the Second International Symposium*: Elsevier, 319.
- Farquharson, C. G., Duckworth, K. and D. W. Oldenburg, 2006. Comparison of integral equation and physical scale modeling of the electromagnetic responses of models with large conductivity contrasts, *Geophysics*, 71, G169-G177.
- Si, H., 2004. TetGen, a quality tetrahedral mesh generator and three-dimensional delaunay triangulator, v1.3 (Technical Report No. 9). Weierstrass Institute for Applied Analysis and Stochastics.
- Saad, Y., 1990. SPARSKIT: a basic tool kit for sparse matrix computations. Report RIACS 90-20, Research Institute for Advanced Computer Science. NASA Ames Research Center.